

Annihilation of heavy-neutral-fermion pairs into monochromatic γ rays and its astrophysical implications

Serge Rudaz

School of Physics and Astronomy, University of Minnesota, Minneapolis, Minnesota 55455

(Received 6 February 1989)

We present estimates for the rates of the processes $\chi\chi \rightarrow \gamma\gamma$ and $\chi\chi \rightarrow V\gamma$, where χ is a heavy-neutral-fermion candidate for galactic cold dark matter and V is a vector quarkonium state $J/\psi(3097)$ or $\Upsilon(9460)$. A discrepancy with a previous estimate of the rate of the photino pair annihilation process $\tilde{\gamma}\tilde{\gamma} \rightarrow \gamma\gamma$ is uncovered and its origin discussed. We explore the possibility that some of the processes considered may be astrophysically significant sources of monochromatic γ -ray lines, in the energy range of a few to a few tens of GeV, for which theoretical estimates of the background γ -ray flux are unfortunately subject to large uncertainties.

I. INTRODUCTION

Of the many new types of particles that have been put forward as candidates to comprise the dark matter of the Universe, the lightest (stable, neutral) superpartner (LSP, generically denoted χ) state appearing in extensions of the standard model with broken supersymmetry has received the most detailed attention, with a wide variety of indirect methods suggested for its detection.¹ One reason for this is that the typical weak-interaction strength of processes involving LSP's leads naturally, in the framework of the big-bang scenario for the evolution of the early Universe, to relic LSP densities that are of the order of the closure density of the present-day Universe: Early calculations of relic LSP densities were done by Goldberg² and Ellis, Hagelin, Nanopoulos, Olive, and Srednicki,³ leading to an essentially continuous updating process by a number of authors, the most recent results of which can be found in an article by Srednicki, Watkins, and Olive.⁴

An attractive method of dark-matter detection is to search for high-energy cosmic rays such as antiprotons, positrons, and γ rays, which could be produced as final states in the annihilation of dark-matter particles in the galactic halo.⁵⁻⁷ In particular, it was suggested⁸⁻¹⁰ that some $\chi\chi$ annihilation processes could lead to very-high-energy (multi-GeV or more), highly monochromatic γ -ray lines that could conceivably be distinguished from the diffuse γ -ray background by means of high-resolution γ -ray telescopes.^{11,12} Two such processes are $\chi\chi \rightarrow V\gamma$ and $\chi\chi \rightarrow \gamma\gamma$, where V is a $J^{PC}=1^{--}$, 3S_1 charmonium (ψ -family) or bottomonium (Υ -family) bound state of a heavy-quark-antiquark pair, respectively, $c\bar{c}$ and $b\bar{b}$. The original estimate presented for the rate of the former type of process by Srednicki, Theisen, and Silk⁸ was quickly revised downward (by an order of magnitude or more) by the present author⁹ whose results were subsequently confirmed by Bergstrom and Snellman.¹⁰ These authors also presented an estimate¹⁰ of the two-photon annihilation process $\tilde{\gamma}\tilde{\gamma} \rightarrow \gamma\gamma$, where $\chi=\tilde{\gamma}$ is a photino, the spin- $\frac{1}{2}$ supersymmetric partner of the photon.

The purpose of this paper is to sharpen previous estimates^{9,10} of the rates of the processes $\chi\chi \rightarrow \gamma\gamma$ and $\chi\chi \rightarrow V\gamma$ as potentially significant astrophysical sources of monochromatic γ -ray lines, for a variety of choices for the cold-dark-matter candidate particle χ . Although in general the LSP is a linear combination of the spin- $\frac{1}{2}$ superpartners of the neutral electroweak gauge bosons γ and Z and of the two types of neutral scalar Higgs particles H_1^0 and H_2^0 , we will consider only two simple possibilities, namely, $\chi=\tilde{\gamma}$ (pure photino) and $\chi=\tilde{H}$ (generic Higgsino), for which the interactions of the hypothetical χ with the known fermions and gauge bosons of the standard model involve the fewest unknown parameters. We note the important point that both $\tilde{\gamma}$ and \tilde{H} are Majorana fermions, namely, that they are identical to their antiparticles, as opposed to the usual case of Dirac fermions in which particle and antiparticle are distinct. This implies in the nonrelativistic limit that a Majorana fermion pair $\chi\chi$ in, say, an s -wave state can only have the pseudoscalar quantum numbers $J^{PC}=0^{-+}$ corresponding to the 1S_0 state (the 3S_1 state is odd under particle-antiparticle conjugation and is, therefore, not allowed). We will also consider the more *ad hoc* possibilities $\chi=\nu_M$ or ν_D , respectively, a heavy Majorana or Dirac neutrino.

We note that our estimate for one particular process, namely, $\tilde{\gamma}\tilde{\gamma} \rightarrow \gamma\gamma$, is in disagreement with that presented by Bergstrom and Snellman,¹⁰ as will be discussed in Sec. II; Secs. III and IV are concerned with rate estimates for $\chi=(\tilde{H}, \nu_M)$ and ν_D , respectively. Finally, in Sec. V, we discuss whether monochromatic γ -ray lines from dark-matter annihilation could be distinguished from the diffuse γ -ray background flux.

II. MONOCHROMATIC PHOTONS FROM PHOTINO ($\tilde{\gamma}$) PAIR ANNIHILATION

The basic interaction vertex, of electromagnetic strength, involves a photino and pairwise all electrically charged particles related by supersymmetry. Thus, the transition $\tilde{\gamma}\tilde{\gamma} \rightarrow \gamma\gamma$ will involve box diagrams such as the ones pictured in Fig. 1, together with those in which the

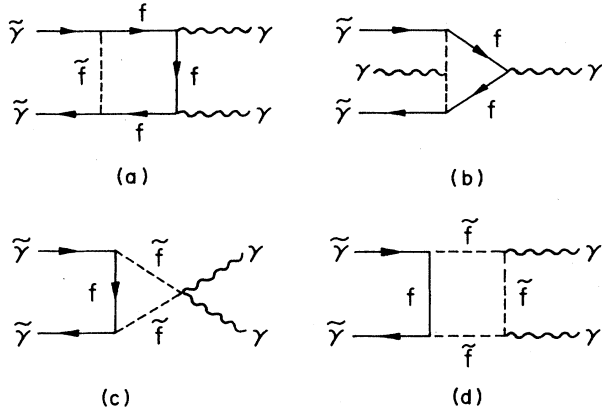


FIG. 1. Typical box diagrams contributing to the transition amplitude for the process $\tilde{\gamma}\tilde{\gamma} \rightarrow \gamma\gamma$. The corresponding diagrams with photon lines interchanged are not shown.

final-state photons are interchanged. In this figure, f denotes the usual leptons and quarks and \tilde{f} (dashed lines) are their respective scalar superpartners: in general there will be many more box graphs, involving virtual charged gauge and Higgs bosons and their superpartners and these will discuss separately. We will at this stage make the following assumption: *all* particles in the theory except for the photon, known fermions (perhaps including the top quark), and the photino itself have masses greater than or equal to M_W , that of the charged weak boson. We will also assume that the masses of all scalar superpartners of known left- and right-handed fermions have one common value $\tilde{M}_L = \tilde{M}_R = \tilde{M}$.

The photinos in the galactic halo are nonrelativistic, with $\beta = v/c \approx 10^{-3}$. The total center-of-mass energy is then $s^{1/2} = 2M_{\tilde{\gamma}}$, and the four-momentum transfer squared from photino to photon is $-M_{\tilde{\gamma}}^2$. The condition that photinos be light as compared to the scale set by \tilde{M} then implies that we are interested in the limit in which all kinematic invariants satisfy $s, |t|, |u| \ll \tilde{M}^2$. In this case, the largest contribution to the convergent box graphs shown in Fig. 1 comes from small loop momenta, and it is reasonable to evaluate the resulting amplitudes in an expansion in inverse powers of the heavy mass \tilde{M} . This can be done in a systematic way, for example, after reducing the calculation of the box graphs to a three-dimensional integral over Feynman parameters. In fact, precisely this exercise has been done for the standard-model process $\nu_l \bar{\nu}_l \rightarrow \gamma\gamma$ in the low-energy limit.¹³ In this case, the result of the calculation of the full box-graph amplitudes is reproduced by simply using the usual effective interaction Lagrangian involving light neutrinos and fermions in the low-energy limit $s \ll M_W^2$ and calculating the resulting pair of fermion triangle diagrams, provided one enforces the constraint of electromagnetic gauge invariance, in the manner first advocated by Rosenberg.¹⁴ We will follow this procedure for the photino annihilation process: in the limit $s \ll \tilde{M}^2$, and in an expansion in inverse powers of \tilde{M}^2 , the calculation should reduce to the evaluation of the $\tilde{\gamma}\tilde{\gamma} \rightarrow \gamma\gamma$ transition using

the usual effective interaction Lagrangian for photinos and light fermions ($m_f \ll \tilde{M}$): namely,^{2,3}

$$\mathcal{L}_{\text{eff}} = \bar{\chi} \gamma^\lambda \gamma_5 \chi \bar{f} \gamma_\lambda (a_f^{\tilde{\gamma}} + b_f^{\tilde{\gamma}} \gamma_5) f, \quad (1)$$

where χ is the photino field and

$$\begin{aligned} a_f^{\tilde{\gamma}} &= 0, \\ b_f^{\tilde{\gamma}} &= (eQ_f)^2 / 2\tilde{M}^2 = (G_F Q_f^2 / \sqrt{2}) (4 \sin^2 \theta_W M_W^2 / \tilde{M}^2), \end{aligned} \quad (2)$$

where eQ_f is the fermion electric charge. The usefulness of the latter expression arises from the numerical coincidence that $\sin^2 \theta_W \approx \frac{1}{4}$ quite accurately. G_F is the Fermi constant: $G_F = 1.16 \times 10^{-5} \text{ GeV}^{-2}$. The resulting matrix element is then

$$\begin{aligned} \mathcal{M}(\tilde{\gamma}\tilde{\gamma} \rightarrow \gamma\gamma) &= \langle 0 | \bar{\chi} \gamma^\lambda \gamma_5 \chi | \tilde{\gamma}(p_1) \tilde{\gamma}(p_2) \rangle \\ &\times \sum_f b_f^{\tilde{\gamma}} \langle \gamma(k_1) \gamma(k_2) | J_{\lambda 5}^f | 0 \rangle_{\text{gi}}, \end{aligned} \quad (3)$$

where the subscript gi reminds us to take only the gauge-invariant piece of the matrix element of the fermionic axial-vector current $J_{\lambda 5}^f = \bar{f} \gamma_\lambda \gamma_5 f$ between the vacuum and the final two-photon state. This condition must be enforced because the diagrams of Fig. 1 (together with those obtained after the interchange of the two final photons) form a gauge-invariant subset of graphs. Note that (3) is of order \tilde{M}^{-2} .

We now dispose of the contribution of the remaining box graphs not shown, involving only heavy ($M \gtrsim M_W$) virtual particles, including gauge and Higgs bosons and their fermions superpartners: In the limit $s \ll M^2$, the effects of all these graphs will amount to the appearance of a *local* effective interaction involving the product of two photino fields and two electromagnetic field-strength tensors (because of gauge invariance) at the same space-time point, typically of the form

$$\mathcal{L}(\text{local}) = \frac{e^4}{16\pi^2} C \bar{\chi}(x) \gamma_5 \chi(x) \epsilon_{\mu\nu\lambda\sigma} F^{\mu\nu}(x) F^{\lambda\sigma}(x). \quad (4)$$

The important point here is that, independent of the particular Lorentz- and gauge-invariant tensor structure which arises, the coefficient C is determined to have dimension of $(\text{mass})^{-3}$ and so, typically, will be of order M^{-3} or $M_{\tilde{\gamma}} M^{-4}, \dots$, etc., where M is the heavy mass: These contributions are all subleading as compared to that of Eq. (3), which is of order \tilde{M}^{-2} . Thus, the transition matrix element for $\tilde{\gamma}\tilde{\gamma} \rightarrow \gamma\gamma$ in the limit $M_{\tilde{\gamma}} \ll M_W$ should be reliably estimated by the expression (3).

The calculation of the gauge-invariant part of the axial-vector current appearing in Eq. (3) was done 25 years ago by Rosenberg,¹⁴ with the result (a color factor $N_c = 3$ should be included when $f = \text{quark}$)

$$\begin{aligned} \langle \gamma(k_1) \gamma(k_2) | J_{\lambda 5}^f | 0 \rangle_{\text{gi}} \\ = - \frac{ie^2 Q_f^2}{\pi^2 s} P_\lambda \epsilon_{\mu\nu\rho\sigma} \epsilon^\mu(k_1) \epsilon^\nu(k_2) k_1^\rho k_2^\sigma I(\xi_f), \end{aligned} \quad (5)$$

where $s = P^2$ is the total center-of-mass energy squared,

with $P = p_1 + p_2 = k_1 + k_2$ the total four-momentum. The dimensionless variable ξ_f is defined to be $\xi_f = 4m_f^2/s$ and $I(\xi_f)$ is a Feynman parametric integral¹⁴

$$I(\xi_f) = \int_0^1 dx \int_0^{1-x} dy \frac{xy}{xy - \xi_f/4} \quad (6)$$

for which the limiting values are

$$I(\xi_f) \xrightarrow{\xi_f \ll 1} \frac{1}{2}, \quad I(\xi_f) \xrightarrow{\xi_f \gg 1} -\frac{1}{6\xi_f}. \quad (7)$$

These two expressions are sufficient to get a rough estimate of the rate; however, the integral in Eq. (5) can in fact be evaluated in closed form (see the Appendix) with the result

$$I(\xi_f) = \frac{1}{2} [1 + \xi_f J(\xi_f)], \quad (8)$$

where

$$J(\xi_f) = \begin{cases} -(\arctan 1/\sqrt{\xi_f-1})^2, & \xi_f \geq 1, \\ \left[\frac{1}{2} \ln \frac{1+\sqrt{1-\xi_f}}{1-\sqrt{1-\xi_f}} - \frac{i\pi}{2} \right]^2, & \xi_f \leq 1. \end{cases} \quad (9)$$

Note that even when $m_f = 0$ one has the result

$$P^\lambda \langle \gamma(k_1) \gamma(k_2) | J_{\mu 5}^f | 0 \rangle \neq 0 \quad (10)$$

which is, of course, the famous chiral anomaly,¹⁵ a result implicit in the work of Rosenberg.¹⁴

It is now straightforward to compute the annihilation cross section times relative velocity for the process $\tilde{\gamma}\tilde{\gamma} \rightarrow \gamma\gamma$, in the limit $s \ll \tilde{M}^2$:

$$\sigma(\tilde{\gamma}\tilde{\gamma} \rightarrow \gamma\gamma) v_{\text{rel}} = \frac{4\alpha^2 M_{\tilde{\gamma}}^2}{\pi^3} \left| \sum_f b_f^{\tilde{\gamma}} Q_f^2 I(\xi_f) \right|^2 \quad (11)$$

again remembering to sum over quark colors. Note that in this expression we have not yet set $s = 4M_{\tilde{\gamma}}^2$, the value appropriate in the nonrelativistic case. A comparison of this result with that of Bergstrom and Snellman¹⁰ shows that they have in fact only retained the part of Eq. (8) proportional to $J(\xi_f)$ [this function is in fact the same as the $F(x)$ given in their Eq. (28)], discarding the constant piece. The ostensible reason for this is that they¹⁰ chose to enforce the conservation of the axial-vector current $\partial^\mu J_{\mu 5}^f = 0$ in the limit $m_f \rightarrow 0$, which is at odds with the requirement of electromagnetic gauge invariance¹³⁻¹⁵ imposed here [cf. Eq. (10)]. As a consequence, the estimate for the rate of the process $\tilde{\gamma}\tilde{\gamma} \rightarrow \gamma\gamma$ presented here will be considerably in excess of that of Ref. 10. Since an exact calculation of the box-graph amplitudes with a realistic superparticle mass spectrum has not yet been done, it is probably best to provisionally consider the results of Ref. 10 and our work as providing, respectively, lower and upper bounds to the rate for $\tilde{\gamma}\tilde{\gamma} \rightarrow \gamma\gamma$. With this caveat borne in mind, we proceed with our analysis.

It is interesting to consider the s dependence of the cross section as given in Eq. (11) in the simple case of only one contributing fermion species f . In the limit $s \ll 4m_f^2 \ll \tilde{M}^2$, the fermion f is itself considered a heavy particle, all box-graph propagators are shrunk to a point

and the amplitude should follow from a local effective interaction similar to that in Eq. (4). In fact, in this limit one finds $\sigma v_{\text{rel}} = O(\alpha^4 M_{\tilde{\gamma}}^2 s^2 / \tilde{M}^4 m_f^4)$, precisely as would be expected from Eq. (4) with $C = O(M_{\tilde{\gamma}} / \tilde{M}^2 m_f^2)$. This rise with s would persist until the regime $4m_f^2 \ll s \ll \tilde{M}^2$ is reached, where one finds $\sigma v_{\text{rel}} = O(\alpha^2 M_{\tilde{\gamma}}^2 / \tilde{M}^4)$ independent of s . Finally, when $4m_f^2, \tilde{M}^2 \ll s$ we expect that, as follows from dimensional analysis, $\sigma v_{\text{rel}} = O(\alpha^4/s)$.

We now specialize to the nonrelativistic case $s = 4M_{\tilde{\gamma}}^2$ and show in Fig. 2 the cross section $\sigma(\tilde{\gamma}\tilde{\gamma} \rightarrow X) v_{\text{rel}}$ as a function of $M_{\tilde{\gamma}}$ for the final states $X = \gamma\gamma$, $J/\psi\gamma$, and $\Upsilon\gamma$, with the latter two radiative quarkonium processes as computed from the formula (12) of Ref. 9 (note that the production of the lowest vector quarkonium state is the dominant process, with that of the corresponding pseudoscalar state having a rate that vanishes by gauge invariance). We have used the values $\tilde{M} = (4 \sin^2 \theta_W)^{1/2} M_W$ and $m_t = 50$ GeV in this figure, both of which correspond essentially to lower limits that follow from experiment. In fact, the result is quite insensitive to the assumed value of m_t , because in the region $M_{\tilde{\gamma}}^2 \ll m_t^2$ the top quark essentially yields a subleading contribution (cf. the discussion above) to the amplitude.

A comparison of these results to the corresponding ones in Ref. 10 shows that the present estimate of the $\gamma\gamma$ cross section is indeed larger for $M_{\tilde{\gamma}} \gtrsim 4$ GeV: the discrepancy amounts to a factor of 50 when $M_{\tilde{\gamma}} = 10$

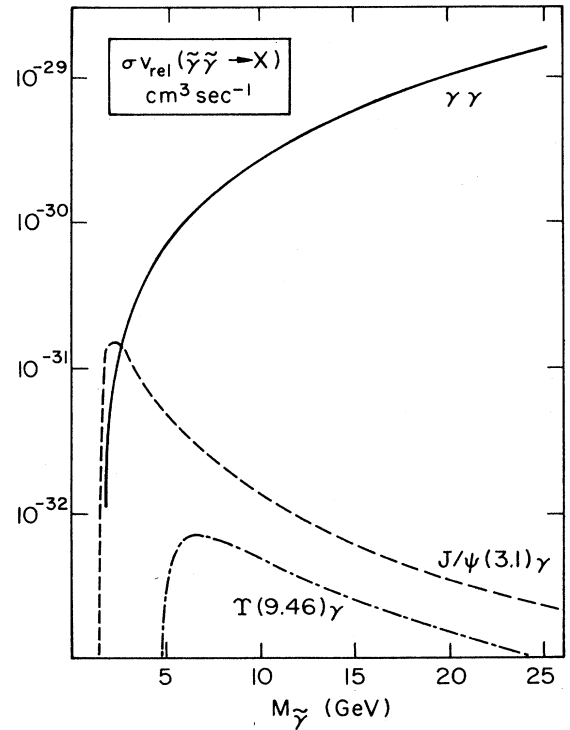


FIG. 2. Cross section times relative velocity for the processes $\tilde{\gamma}\tilde{\gamma} \rightarrow \gamma\gamma$, $J/\psi\gamma$, and $\Upsilon\gamma$ in the nonrelativistic limit, as a function of photino mass, with $\tilde{M} = 2 \sin \theta_W M_W$.

GeV, for example. We are, however, in qualitative agreement with the authors of Ref. 10 on two points; first, the $\gamma\gamma$ mode dominates by far the radiative quarkonium modes, and, second, the rate is proportional to $M_{\tilde{\gamma}}^2$. As we are in the regime $4m_f^2 \ll s \ll \tilde{M}^2$ for all fermions except the top quark, we expect our results to be valid for $M_{\tilde{\gamma}}^2 \ll \tilde{M}^2/4$, and, hence, given $\tilde{M} \simeq M_W$, we have chosen to draw the $\gamma\gamma$ curve up to a value $M_{\tilde{\gamma}} \simeq 25\text{--}30$ GeV or so. An extrapolation up to $M_{\tilde{\gamma}} \approx \tilde{M}/2 \simeq 40$ GeV should still give a reasonable estimate but one should go no farther as the rate must eventually turn over and attain its asymptotic form $O(\alpha^4/s)$ as s increases beyond \tilde{M}^2 .

Values of \tilde{M} larger than M_W are easily accommodated: simply rescale the three curves in Fig. 2 by a factor $(4 \sin^2 \theta_W M_W^2 / \tilde{M}^2)^2$, and the $\gamma\gamma$ process estimate should then be reliable to about $M_{\tilde{\gamma}} \simeq \tilde{M}/2$ or a bit less. One should also remember that in the region $m_t \lesssim M_{\tilde{\gamma}} \lesssim \tilde{M}/2$, including top-quark effects (now t is a ‘‘light’’ particle) leads to a further 30% increase in the $\gamma\gamma$ annihilation cross section. One last important point must be noted as it regards the selection of a particular value for \tilde{M} : given such a value, there are both upper and lower limits on $M_{\tilde{\gamma}}$ that follow from the requirement that photinos be cosmologically relevant and so can in fact be consistent dark-matter candidates. On the one hand, at fixed \tilde{M} , if photinos are too light, their annihilation rate into fermions will be too small (it is then essentially proportional to m_f^2) to efficiently reduce their number before freeze-out, and there will be too many of them left: requiring a relic density to not exceed the present-day closure implies²⁻⁴ $M_{\tilde{\gamma}} \gtrsim 5$ GeV or so for $\tilde{M} = O(M_W)$. On the other hand, if photinos are too heavy, it turns out their annihilation before freeze-out can be so efficient that their relic mass density dwindles into cosmological insignificance: again for $\tilde{M} = O(M_W)$ this happens for $M_{\tilde{\gamma}} \gtrsim 30$ GeV beyond which point the cosmic photino density can be roughly estimated to be below 10% of the closure density.

Finally, we note that as compared to the annihilation process into light fermions $\tilde{\gamma}\tilde{\gamma} \rightarrow f\bar{f}$ with a cross section $\sigma(\tilde{\gamma}\tilde{\gamma} \rightarrow f\bar{f})_{v_{\text{rel}}} \simeq 2.3 \times 10^{-27} (4 \sin^2 \theta_W M_W^2 / \tilde{M}^2)^2 \text{ cm}^3 \text{ sec}^{-1}$ in the nonrelativistic limit, and for $m_b < M_{\tilde{\gamma}} < m_t$, the reaction $\tilde{\gamma}\tilde{\gamma} \rightarrow \gamma\gamma$ has a branching ratio that does not exceed (at its peak value around $M_{\tilde{\gamma}} \lesssim \tilde{M}/2$) a fraction of a percent or so. However, as pointed out by Bergstrom and Snellman,¹⁰ one can also estimate the rate for the two-gluon annihilation process $\tilde{\gamma}\tilde{\gamma} \rightarrow g^a g^b$, summed over gluon colors a, b . The results is, for $m_b \lesssim M_{\tilde{\gamma}} < m_t$,

$$\frac{\sigma(\tilde{\gamma}\tilde{\gamma} \rightarrow gg)}{\sigma(\tilde{\gamma}\tilde{\gamma} \rightarrow \gamma\gamma)} \simeq 2 \left(\frac{\alpha_s}{\alpha} \right)^2 \frac{\left| \sum_q Q_q^2 I(\xi_q) \right|^2}{\left| \sum_f Q_f^4 3^{\delta_{f_q}} I(\xi_f) \right|^2} \simeq 100 \left(\frac{\alpha_s}{0.19} \right)^2,$$

where all required color factors are explicitly shown. Remarkably, the gluon-gluon annihilation cross section of photino pairs in the nonrelativistic limit appears to be of the same order of magnitude as that into fermion-antifermion pairs over much of the range of $M_{\tilde{\gamma}}$ considered here. The further astrophysical and cosmological implications of this result will not be considered here.

III. MONOCHROMATIC PHOTONS FROM HIGGSINO (\tilde{H}) AND MAJORANA NEUTRINO (ν_M) PAIR ANNIHILATION

An alternative to the photino as a possible LSP candidate is the so-called generic or pure Higgsino \tilde{H} . A minimal broken supersymmetric extension of the standard model will typically involve neutral-Higgs-scalar particles H_1^0 and H_2^0 , with corresponding vacuum expectation values v_1 and v_2 . As long as the quantity

$$\cos 2\beta = \frac{v_1^2 - v_2^2}{v_1^2 + v_2^2} \quad (12)$$

is slightly different from, but still of order of, unity, then the trilinear coupling $\tilde{H}f\bar{f}$ of a generic Higgsino \tilde{H} to a fermion f and its scalar superpartner \tilde{f} is suppressed by a factor of order m_f/\tilde{M} as compared to a typical gauge coupling (for example, e). Under these conditions, the contributions of box graphs analogous to those of Fig. 1 to the process $\tilde{H}\tilde{H} \rightarrow \gamma\gamma$ are suppressed as compared to the dominant part of the amplitude involving Z^0 exchange pictured in Fig. 3. This is once again given by the gauge-invariant matrix element of the fermionic axial-vector current and now takes the form

$$\begin{aligned} \mathcal{M}(\tilde{H}\tilde{H} \rightarrow \gamma\gamma) &= \langle 0 | \bar{\chi} \gamma^\lambda \gamma_5 \chi | \tilde{H}(p_1) \tilde{H}(p_2) \rangle \\ &\times \left[\frac{g_{\lambda\rho} - P_\lambda P_\rho / M_Z^2}{1 - s/M_Z^2 - i\Gamma_Z/M_Z} \right] \\ &\times \sum_f b_f^{\tilde{H}} \langle \gamma(k_1) \gamma(k_2) | \bar{f} \gamma^\rho \gamma_5 f | 0 \rangle_{\text{gi}} \quad (13) \end{aligned}$$

including the Z -boson propagator with finite width Γ_Z in the unitary gauge (in the limit $s \ll M_Z^2$ this is just $g_{\lambda\rho}$) and $b_f^{\tilde{H}}$ is the analog for Higgsinos of the coupling $b_f^{\tilde{\gamma}}$ defined in Eq. (1). This is given by

$$b_f^{\tilde{H}} = -\frac{G_F}{\sqrt{2}} T_{3L}^f \cos 2\beta \quad (14)$$

with $\cos 2\beta$ of order unity as mentioned earlier and T_{3L}^f is the third component of the weak isospin of the left-

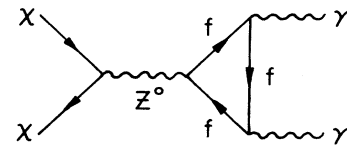


FIG. 3. Diagram contributing to the transition amplitude for the process $\chi\chi \rightarrow \gamma\gamma$ with χ either a heavy generic Higgsino, Majorana neutrino, or Dirac neutrino. There is also a corresponding graph with crossed photon lines.

handed fermions: namely, $T_{3L}^f = +\frac{1}{2}$ for $f = u, c, t$ and $T_{3L}^f = -\frac{1}{2}$ for $f = e, \mu, \tau, d, s, b$. There is no contribution from the fermionic vector current to the matrix element because of C invariance.

The expression (13) applies without approximation to the process $\nu_M \nu_M \rightarrow \gamma\gamma$, where ν_M is a Majorana neutrino, defined to have standard-model neutrino couplings to the Z boson, and with

$$b_f^\nu = -\frac{G_F}{\sqrt{2}} T_{3L}^f. \quad (15)$$

No factor of $\cos 2\beta$ enters, and there are no box graphs to consider in this case. A heavy, stable, Majorana neutrino does not fit as naturally as a photino or Higgsino in non-trivial extensions of the standard model, however.

Inserting the expression (5) with its explicit factor P^ρ into Eq. (13) gives rise to the quantity

$$P^\rho (g_{\lambda\rho} - P_\lambda P_\rho / M_Z^2) = P_\lambda (1 - s/M_Z^2) \quad (16)$$

so that the Z -exchange amplitude actually vanishes on resonance, in agreement with a well-known theorem forbidding the decay of any odd spin particle into two photons.

The cross section for the process $\chi\chi \rightarrow \gamma\gamma$ when $\chi = \tilde{H}$ or ν_M is now given by Eq. (11) with the replacement

$$b_f^\chi \rightarrow b_f^\chi (1 - s/M_Z^2) (1 - s/M_Z^2 - i\Gamma_Z/M_Z)^{-1}. \quad (17)$$

This is shown as a function of M_χ in the nonrelativistic limit $s = 4M_\chi^2 \ll M_Z^2$, where Z -propagator effects are negligible, and with $m_t = 50$ GeV, in Fig. 4. We have

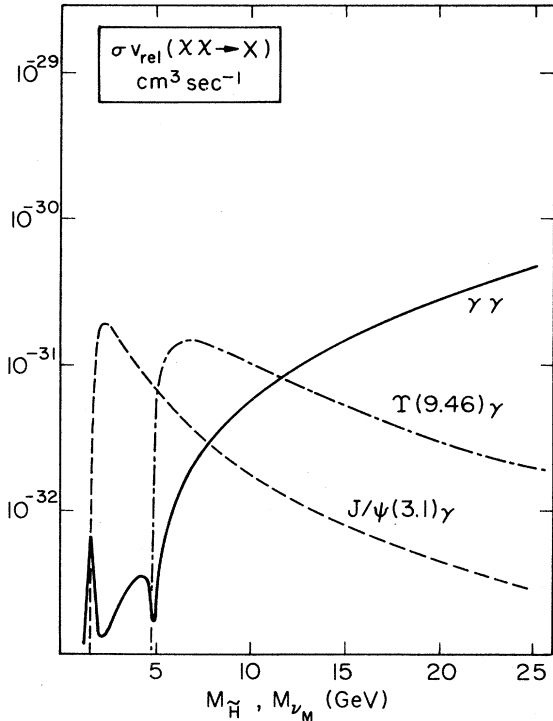


FIG. 4. Cross section times relative velocity for the process $\chi\chi \rightarrow \gamma\gamma$, $J/\psi\gamma$, and $\Upsilon\gamma$ in the nonrelativistic limit, for $\chi =$ generic Higgsino or Majorana neutrino, as a function of the χ mass.

chosen $\cos^2 2\beta \simeq 1$ so that, in fact, the same curve applies to both cases $\chi = \tilde{H}$ or ν_M ; the Higgsino curve can be rescaled to accommodate a lower value for $\cos^2 2\beta$. Also shown are the radiative quarkonium processes $\chi\chi \rightarrow J/\psi\gamma$ or $\Upsilon\gamma$. This time, there is not much variation in the magnitude of the respective cross sections, although the $\gamma\gamma$ process does dominate over the quarkonium ones above $M_\chi = 10$ GeV. The reason for the suppression of the $\gamma\gamma$ annihilation rate for $\chi = \tilde{H}$, ν_M as compared to that for $\chi = \tilde{\nu}$ is easily traced to the corresponding values of b_f^χ , Eqs. (2), (14), and (15). The factors that enter the rate at a given M_χ are approximately given as a sum over "light" fermions such that $M_\chi \gtrsim m_f$:

$$\sum_f' b_f^\chi Q_f^2 \sim \begin{cases} \sum_f' Q_f^4, & \chi = \tilde{\nu}, \\ \sum_f' T_{3L}^f Q_f^2, & \chi = \tilde{H}, \nu_M, \end{cases} \quad (18)$$

where the prime indicates the restriction to light fermions. For photinos, the sum involves positive-definite quantities, while in the other two cases there are cancellations among fermions with opposite values of T_{3L}^f : in fact, for $M_\chi \gtrsim m_t$, the sum extends over *all* species of quarks and leptons, for which one has the famous relation (remember the quark color factor)

$$\sum_{\text{all } f} T_{3L}^f Q_f^2 = 0 \quad (19)$$

which guarantees the cancellation of all anomalies in gauged chiral currents in the standard model. Thus, we see that it is only by virtue of the effective decoupling of the top quark when $M_\chi \lesssim m_t$ that the Z^0 -boson-exchange contribution to the process $\chi\chi \rightarrow \gamma\gamma$, when $\chi = \tilde{H}$ or ν_M , is nonvanishing. For $M_\chi \gtrsim m_t$, only the much smaller box graphs contribute to $\tilde{H}\tilde{H} \rightarrow \gamma\gamma$ while $\nu_M \nu_M \rightarrow \gamma\gamma$ has a vanishing rate. It is interesting to note that by virtue of Eq. (19) our calculation of the rate for $\chi\chi \rightarrow \gamma\gamma$ via Z exchange will agree with that performed using the prescription of Bergstrom and Snellman,¹⁰ which amounts to discarding the "anomaly contribution."

However, we must now remember the limits on M_χ set by the requirement of cosmological relevance⁴ which are quite restrictive: in fact, one need only consider the range $5 \text{ GeV} \lesssim M_\chi \lesssim 25 \text{ GeV}$ for $\chi = \tilde{H}$ or ν_M .

IV. MONOCHROMATIC PHOTONS FROM THE PAIR ANNIHILATION OF HEAVY DIRAC NEUTRINOS (ν_D)

Finally, we consider the case $\chi = \nu_D$, a heavy Dirac neutrino: such a particle must not mix with the known light Dirac neutrinos to ensure its stability over cosmological times scales. We shall simply define ν_D through its interactions with known fermions, assumed to proceed only via the Z^0 -exchange graph, corresponding in the local limit $s \ll M_Z^2$ to the effective interaction

$$\mathcal{L}_{\text{eff}} = \bar{\nu}_D \gamma^\lambda (1 - \gamma_5) \nu_D \bar{f} \gamma_\lambda (a_f^\nu + b_f^\nu \gamma_5) f. \quad (20)$$

This differs from the analogous quantity for Majorana particles [cf. Eq. (1)] by the presence of a piece involving the vector current $\bar{\nu}_D \gamma^\lambda \nu_D$, an object that vanishes identi-

cally for Majorana fermions. We will take the standard-model values

$$a_f^v = \frac{G_F}{\sqrt{2}}(T_{3L}^f - 2Q_f \sin^2 \theta_w), \quad b_f^v = -\frac{G_F}{\sqrt{2}} T_{3L}^f \quad (21)$$

which also apply when considering Majorana neutrinos [cf. Eq. (15)]: Q_f is the fermion electric charge in units of that of the proton.

The amplitude for $\nu_D \bar{\nu}_D \rightarrow \gamma \gamma$ is precisely of the same form as for $\nu_M \bar{\nu}_M \rightarrow \gamma \gamma$: indeed, the explicit factor of P_λ in Eq. (5) gives rise to a vanishing contribution from the vector part of the Dirac neutrino current, since

$$P_\lambda \langle 0 | \bar{\nu}_D \gamma^\lambda \nu_D | \nu_D(p_1) \bar{\nu}_D(p_2) \rangle = 0 \quad (22)$$

using the Dirac equation. Next we remember that

$$\langle 0 | \bar{\nu}_D \gamma^\lambda \gamma_5 \nu_D | \nu_D \bar{\nu}_D \rangle = \frac{1}{2} \langle 0 | \bar{\nu}_M \gamma^\lambda \gamma_5 \nu_M | \nu_M \bar{\nu}_M \rangle \quad (23)$$

so we immediately conclude

$$\sigma(\nu_D \bar{\nu}_D \rightarrow \gamma \gamma) = \frac{1}{4} \sigma(\nu_M \bar{\nu}_M \rightarrow \gamma \gamma). \quad (24)$$

Next we consider the radiative quarkonium processes: the calculation is done by the methods of Refs. 9 and 10. The presence of the vector current $\bar{\nu}_D \gamma^\lambda \nu_D$ in the effective Lagrangian leads to the following differences as compared to the Majorana case: first, longitudinally polarized vector quarkonia can be produced in the reaction $\nu_D \bar{\nu}_D \rightarrow V \gamma$, and, second, the radiative production of

pseudoscalar (0^{-+}) quarkonia $P = \eta_c, \eta_b$ can now proceed. We recall that both of these were forbidden in the nonrelativistic Majorana case where the initial $\chi \chi$ state is purely pseudoscalar, because of angular momentum conservation and gauge invariance, respectively.

As a consequence of the first point, there is an enhancement in the cross section for $\nu_D \bar{\nu}_D \rightarrow V \gamma$ as compared to that for $\nu_M \bar{\nu}_M \rightarrow \gamma \gamma$ for larger values of M_ν , the heavy Dirac neutrino mass: in fact, we find

$$\sigma(\nu_D \bar{\nu}_D \rightarrow V \gamma) = \frac{1}{2} (1 + 2M_\nu^2 / M_V^2) \sigma(\nu_M \bar{\nu}_M \rightarrow V \gamma) \quad (25)$$

in agreement with Bergstrom and Snellman.¹⁰

Figure 5 shows the rates for the processes $\nu_D \bar{\nu}_D \rightarrow \gamma \gamma$, $J/\psi \gamma$, and $\Upsilon \gamma$, as obtained from Eqs. (24) and (25): we see that the $\gamma \gamma$ process is much suppressed as compared to radiative quarkonium production, whose rates are essentially independent of M_ν . Note that the criterion of cosmological relevance restricts⁴ the mass of heavy Dirac neutrino to the range $5 \text{ GeV} \lesssim M_\nu \lesssim 20 \text{ GeV}$ or so.

Finally, the rate for the radiative production of the pseudoscalar ($Q\bar{Q}$) quarkonium relative to that of the corresponding vector state can be estimated to be¹⁰

$$\frac{\sigma v_{\text{rel}}(\nu_D \bar{\nu}_D \rightarrow P \gamma)}{\sigma v_{\text{rel}}(\nu_D \bar{\nu}_D \rightarrow V \gamma)} \lesssim \left[\frac{a_Q^v}{b_Q^v} \right]^2 \quad (26)$$

which amounts to about 11% for charmonium and 44% for bottomonium.

V. γ -RAY LINES FROM DARK-MATTER ANNIHILATION IN THE GALACTIC HALO

The processes $\chi \chi \rightarrow \gamma \gamma$ and $\chi \chi \rightarrow V \gamma$ give rise to monochromatic photons of respective energies $E_\gamma = M_\chi$ and $M_\chi - M_V^2 / 4M_\chi$, subject only to Doppler broadening $\Delta E_\gamma / E_\gamma = \beta \approx 10^{-3}$, the typical velocity of halo dark-matter particles. The expected line flux, due to a particular process, in the direction defined by galactic latitude and longitude (θ, ϕ) will be^{5,16}

$$F_\gamma(\theta, \phi) (\text{cm}^{-2} \text{sec}^{-1} \text{sr}^{-1}) = \frac{1}{4\pi} \sigma v_{\text{rel}} N_\gamma \int_0^\infty dr(\theta, \phi) n_\chi^2(r), \quad (27)$$

where N_γ is the number of photons emitted in the annihilation process, and the line of sight integral is over the square of the number density of the χ particles in the galactic halo, $n_\chi = \rho_\chi / M_\chi$. The galactic dark-matter halo density $\rho_\chi(R)$, with R measured from the galactic center is taken to have the simple form

$$\rho_\chi(R) = \rho_0 \frac{R_0^2 + a^2}{R^2 + a^2}, \quad (28)$$

where ρ_0 is the local density of dark matter, R_0 is the distance of the solar system to the galactic center, and a is the halo core radius. Typical values for these parameters are

$$\rho_0 = 0.4 \text{ GeV cm}^{-3}, \quad R_0 \approx a \approx 8 \text{ kpc},$$

none of which are known to better than, say 10% (see

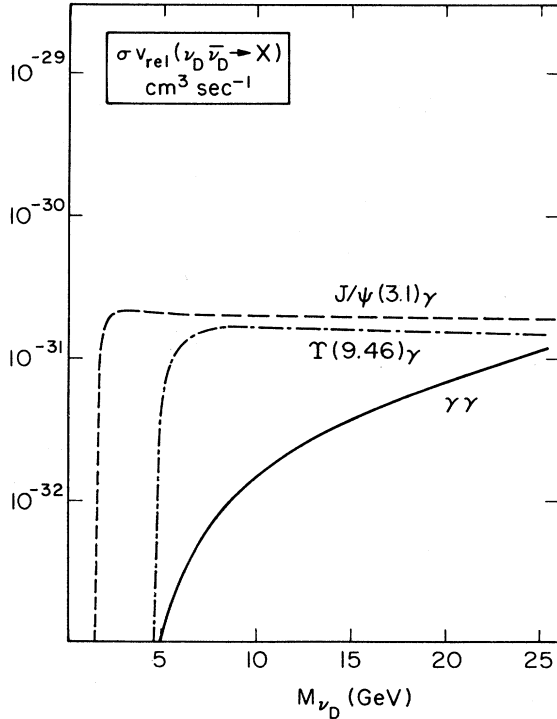


FIG. 5. Cross section times relative velocity for the process $\nu_D \bar{\nu}_D \rightarrow \gamma \gamma$, $J/\psi \gamma$, and $\Upsilon \gamma$ in the nonrelativistic limit, as a function of the heavy Dirac neutrino mass.

Ref. 1 for a discussion). With these values, the simple spherical distribution in Eq. (28) simply encodes the observational result that it is only for $R \gtrsim a$ that the dark-matter density is of the same order as, or larger than, that of luminous matter, with the behavior $\rho_\chi \sim R^{-2}$ leading to flat rotation curves. The photon line flux can then be reexpressed as

$$F_\gamma(\theta, \phi) = \frac{1}{4\pi} \sigma v_{\text{rel}} N_\gamma \left[\frac{\rho_0}{M_\chi} \right]^2 a L(\theta, \phi), \quad (29)$$

where the line-of-sight integral $L(\theta, \phi)$ is now dimensionless. Numerically,

$$F_\gamma(\theta, \phi) = 2 \times 10^{-12} N_\gamma \rho_4^2 M_4^{-2} (\sigma v)_{31} \times a_8 L(\theta, \phi) \text{ cm}^{-2} \text{sec}^{-1} \text{sr}^{-1} \quad (30)$$

with the various quantities normalized to benchmark values: $\rho_4 = \rho_0 / 0.4 \text{ GeV cm}^{-3}$, $M_4 = M_\chi / 4 \text{ GeV}$, $(\sigma v)_{31} = (\sigma v_{\text{rel}}) / 10^{-31} \text{ cm}^3 \text{sec}^{-1}$, and $a_8 = a / 8 \text{ kpc}$. For high galactic latitudes, $\theta \simeq 90^\circ$ (also referred to as the galactic pole), the line-of-sight integral is a factor of order unity^{5,16} and one may guess that it is in that direction that the diffuse γ -ray background of galactic origin is likely to be lowest.

In fact, there are no measurements of the diffuse γ -ray background flux in the energy range considered here: estimates of this background must rely on calculation and extrapolations of lower-energy data. On the one hand, the galactic component of the γ -ray background above $E_\gamma \geq 1 \text{ GeV}$ is predominantly comprised of photons from the decay of π^0 mesons produced as secondaries in collisions of primary-cosmic-ray protons with the interstellar medium. This can be fairly reliably estimated and for high galactic latitudes one expects^{17,18}

$$\frac{dN}{dE_\gamma}(\text{pole}) \simeq 2 \times 10^{-8} \times (E_\gamma / 4 \text{ GeV})^{-2.7} \text{ cm}^{-2} \text{sec}^{-1} \text{sr}^{-1} \text{GeV}^{-1}. \quad (31)$$

On the other hand, the origin of the extragalactic (isotropic) γ -ray flux is not well understood and one must rely on extrapolations of the COS-B and SAS-2 satellite data which only extend to a few hundred MeV. Different analyses (see Ref. 12 and references therein) of these data lead to inconclusive results as regards differential spectral index and magnitude relative to the galactic flux shown above: accordingly, we shall take the galactic spectrum in Eq. (31) as a lower bound on the diffuse γ -ray background flux.

A modern detector such as ASTROGAM¹² will have an energy resolution of about 1%: $\Delta E_\gamma \simeq 10^{-2} E_\gamma$. Thus, comparing signal to background at high galactic latitude we find

$$\frac{F_\gamma(\text{pole})}{\Delta E_\gamma (dN/dE_\gamma)(\text{pole})} \lesssim 3 \times 10^{-3} N_\gamma \rho_4^2 M_4^{-2} (\sigma v)_{31} a_8 E_4^{1.7} \quad (32)$$

with $E_4 = E_\gamma / 4 \text{ GeV}$. The most favorable reaction is $\tilde{\gamma}\tilde{\gamma} \rightarrow \gamma\gamma$, for which $N_\gamma = 2$ and $E_\gamma = M_\tilde{\gamma}$. Using the parametrization

$$(\sigma v)_{31} \simeq 4 M_4^2 (4 \sin^2 \theta_W M_W^2 / \tilde{M}^2)^2 \quad (33)$$

appropriate to that reaction, and valid for $M_4 \geq 1$, we get the best case signal-to-background ratio

$$\frac{F_\gamma(\text{pole}; \tilde{\gamma}\tilde{\gamma} \rightarrow \gamma\gamma)}{\Delta E_\gamma (dN/dE_\gamma)(\text{pole})} \lesssim 2.5 \times 10^{-2} \rho_4^2 M_4^{1.7} a_8 \quad (34)$$

with $\tilde{M} \simeq M_W$. This favors larger photino masses (provided $M_\tilde{\gamma} \lesssim \tilde{M}/2$) and reaches a value of order unity when $M_\tilde{\gamma} \simeq 30 \text{ GeV}$ or so, at the edge of cosmological relevance: note that the line flux itself is actually independent of $M_\tilde{\gamma}$, and with an area \times efficiency factor of $7000 \text{ cm}^2 \text{sr}$ as for ASTROGAM¹² one expects a few events per year. Of course, any improvement in the detector energy resolution over and above the nominal value of 1% will enhance the signal.

We may also consider the monochromatic γ -ray flux from the galactic center that could arise from the annihilation of χ particles comprising the dark-matter component of the galactic spheroid.^{19,20} Following Stecker,²⁰ we adopt the model of Ipser and Sikivie²¹ as a realistic model of a dark-matter source in the galactic center. In this model, the source is a spherical volume of radius $R_s = 150 \text{ pc}$, and with an average density squared of $\langle \rho_\chi^2 \rangle \simeq (120 \text{ GeV cm}^{-3})^2$. Thus, as viewed from the solar system, one looks at a source of angular size of about 1° in the direction of the galactic center. The expected monochromatic photon line flux is then

$$F_\gamma(\text{spheroid}) = \frac{N_\gamma}{4\pi R_0^2} \langle \rho_\chi^2 \rangle M_\chi^{-2} V_s \sigma v_{\text{rel}}, \quad (35)$$

where V_s is the spheroid volume and $R_0 \simeq 8 \text{ kpc}$ the distance to the galactic center. Numerically, one finds a flux of about

$$F_\gamma(\text{spheroid}) \simeq 5 \times 10^{-12} N_\gamma M_4^{-2} (\sigma v)_{31} \text{ cm}^{-2} \text{sec}^{-1} \quad (36)$$

subject to considerable uncertainty, reflecting mainly that of the dark-matter spheroid parameters. Again looking at the most favorable reaction, $\tilde{\gamma}\tilde{\gamma} \rightarrow \gamma\gamma$ we finally arrive at the estimate (for $\tilde{M} \simeq M_W$),

$$F_\gamma(\text{spheroid}; \tilde{\gamma}\tilde{\gamma} \rightarrow \gamma\gamma) \simeq 4 \times 10^{-11} \text{ cm}^{-2} \text{sec}^{-1} \quad (37)$$

independent of $M_\tilde{\gamma} \lesssim \tilde{M}/2$, again corresponding to a few events per year.

These estimates suggest that a dark-matter search via monochromatic γ rays is a realistic goal for future space-borne γ -ray telescopes with high angular and energy resolution. Note that the rate estimates for reactions other than $\tilde{\gamma}\tilde{\gamma} \rightarrow \gamma\gamma$, while hardly encouraging in this respect, do strongly depend on the assumed couplings of the χ candidates to known particles, and may be enhanced (or suppressed, for that matter) for other plausible choices of these couplings.

ACKNOWLEDGMENTS

It is a pleasure to thank Larry Carson and Floyd Stecker for helpful consultations. This work was supported in part by the Department of Energy, under Contract No. DE-AC02-83ER-40105, and by the Presidential Young Investigator Program.

APPENDIX: CALCULATION OF THE VVA FERMION TRIANGLE GRAPH FOR $m_f \neq 0$

Following the pioneering work of Rosenberg,¹⁴ we see that the calculation of the gauge-invariant VVA fermion triangle graph with both external photons on shell reduces to the evaluation of the Feynman parametric integral

$$I(\xi) = \int_0^1 dx \int_0^{1-x} dy \frac{xy}{xy - \xi/4}, \quad (\text{A1})$$

where $\xi = 4m_f^2/s$ and s is the total center-of-mass energy squared. Integrating over y gives

$$I(\xi) = \frac{1}{2} + \frac{\xi}{4} \int_0^1 \frac{dx}{x} \ln[1 - 4x(1-x)/\xi] = \frac{1}{2}[1 + \xi J(\xi)]. \quad (\text{A2})$$

To evaluate $J(\xi)$, use the following technique. Differentiating with respect to ξ , obtain

$$\frac{dJ}{d\xi} = \frac{1}{2\xi} \int_0^1 dx \frac{1-x}{x^2 - x + \xi/4} \quad (\text{A3})$$

which by the usual substitution $y = x - \frac{1}{2}$ is readily evaluated for $\xi > 1$ and $\xi < 1$ separately:

$$\frac{dJ}{d\xi} = \frac{1}{\xi\sqrt{\xi-1}} \arctan 1/\sqrt{\xi-1}, \quad \xi > 1, \quad (\text{A4})$$

$$\frac{dJ}{d\xi} = \frac{-1}{2\xi\sqrt{\xi-1}} \left[\ln \frac{1 + \sqrt{1-\xi}}{1 - \sqrt{1-\xi}} - i\pi \right], \quad \xi < 1. \quad (\text{A5})$$

It now remains simply to integrate these expressions over ξ : for $\xi > 1$, the substitution $\theta = \arctan 1/\sqrt{\xi-1}$ gives

$$J(\xi) = -2 \int \theta d\theta = -\theta^2 + C \quad (\text{A6})$$

where C is a constant of integration to be fixed by the behavior of $I(\xi)$ as $\xi \rightarrow \infty$. In fact, in that limit, directly from (A1),

$$I(\xi) = -\frac{1}{6\xi} + O(1/\xi^2).$$

Consideration of (A6) in the limit $\xi \rightarrow \infty$, together with (A2) readily leads to $C = 0$.

The case $\xi < 1$ is dealt with similarly: rewrite (A5) as

$$\frac{dJ}{d\xi} = -\frac{1}{\xi\sqrt{1-\xi}} (\operatorname{arctanh} \sqrt{1-\xi} - i\pi/2). \quad (\text{A7})$$

The change of variables $\psi = \operatorname{arctanh} \sqrt{1-\xi}$ now gives immediately

$$J(\xi) = 2 \int d\psi (\psi - i\pi/2) = \psi^2 - i\pi\psi + C', \quad (\text{A8})$$

where the constant of integration C' is to be fixed by requiring continuity at $\xi = 1$: this is easily seen to lead to $C' = -\pi^2/4$.

To summarize, $I(\xi)$ has now been expressed in a closed form, as

$$I(\xi) = \frac{1}{2}[1 + \xi J(\xi)]$$

with

$$J(\xi) = -(\arctan 1/\sqrt{\xi-1})^2, \quad \xi \geq 1 \\ = \left[\frac{1}{2} \ln \frac{1 + \sqrt{1-\xi}}{1 - \sqrt{1-\xi}} - \frac{i\pi}{2} \right]^2, \quad \xi \leq 1. \quad (\text{A9})$$

Note that a very similar parametric integral enters in the calculation of the amplitude for the decay of a Higgs boson into a gluon pair, the inverse process of which is of great interest for the production of Higgs bosons at hadron colliders.

¹J. R. Primack, D. Seckel, and B. Sadoulet, *Annu. Rev. Nucl. Part. Sci.* **38**, 751 (1988).
²H. Goldberg, *Phys. Rev. Lett.* **50**, 1419 (1983).
³J. Ellis, J. S. Hagelin, D. V. Nanopoulos, K. Olive, and M. Srednicki, *Nucl. Phys.* **B238**, 453 (1984).
⁴M. Srednicki, R. Watkins, and K. Olive, *Nucl. Phys.* **B310**, 693 (1988).
⁵J. E. Gunn, B. W. Lee, I. Lerche, D. N. Schramm, and G. Steigman, *Astrophys. J.* **223**, 1015 (1978); F. W. Stecker, *ibid.* **223**, 1032 (1978).
⁶Ya. B. Zeldovich, A. A. Klypin, M. Yu. Khlopov, and V. M. Chechetkin, *Yad. Fiz.* **31**, 1286 (1980) [*Sov. J. Nucl. Phys.* **31**, 664 (1980)].
⁷J. Silk and M. Srednicki, *Phys. Rev. Lett.* **53**, 624 (1984); F. W. Stecker, S. Rudaz, and T. F. Walsh, *ibid.* **55**, 2622 (1985); S. Rudaz and F. W. Stecker, *Astrophys. J.* **325**, 16 (1988).
⁸M. Srednicki, S. Theisen, and J. Silk, *Phys. Rev. Lett.* **56**, 263 (1986); **56**, 1883(E) (1986).
⁹S. Rudaz, *Phys. Rev. Lett.* **56**, 2128 (1986).
¹⁰L. Bergstrom and H. Snellman, *Phys. Rev. D* **37**, 3737 (1988).

¹¹D. Eichler and J. H. Adams, *Astrophys. J.* **317**, 551 (1987).
¹²ASTROGAM (Very Energetic γ -Ray Astronomy Experiment using the ASTROMAG Facility), a proposal to the National Aeronautics and Space Administration for a Space Station-Attached Payload, J. H. Adams, Principal Investigator (unpublished).
¹³V. K. Cung and M. Yoshimura, *Nuovo Cimento* **29A**, 557 (1975).
¹⁴L. Rosenberg, *Phys. Rev.* **129**, 2786 (1963).
¹⁵S. L. Adler, *Phys. Rev.* **177**, 2426 (1969); J. S. Bell and R. Jackiw, *Nuovo Cimento* **60A**, 47 (1969); see, also, A. D. Dolgov and V. I. Zakharov, *Nucl. Phys.* **B27**, 525 (1971).
¹⁶M. S. Turner, *Phys. Rev. D* **34**, 1921 (1986).
¹⁷F. W. Stecker, in *The Large Scale Characteristics of the Galaxy*, edited by W. B. Burton (Reidel, Dordrecht, 1979), p. 475.
¹⁸C. D. Dermer, *Astron. Astrophys.* **157**, 223 (1986).
¹⁹J. Silk and H. Bloemen, *Astrophys. J. Lett.* **313**, L47 (1987).
²⁰F. W. Stecker, *Phys. Lett. B* **201**, 529 (1988).
²¹J. Ipser and P. Sikivie, *Phys. Rev. D* **35**, 3695 (1987).